

Novel Internal Target for Electron Scattering off Unstable Nuclei

M. Wakasugi,¹ T. Emoto,¹ Y. Furukawa,^{2,*} K. Ishii,³ S. Ito,¹ T. Koseki,^{1,†} K. Kurita,³ A. Kuwajima,² T. Masuda,^{3,‡} A. Morikawa,³ M. Nakamura,¹ A. Noda,⁴ T. Ohnishi,¹ T. Shirai,⁴ T. Suda,¹ H. Takeda,¹ T. Tamae,² H. Tongu,⁴ S. Wang,¹ and Y. Yano¹

¹RIKEN Nishina Center, Wako, Saitama 351-0198, Japan

²Laboratory of Nuclear Science, Tohoku University, Sendai, Miyagi 982-0826, Japan

³Department of Physics, Rikkyo University, Toshima, Tokyo 171-8501, Japan

⁴Institute of Chemical Research, Kyoto University, Uji, Kyoto 611-0011, Japan

(Received 9 November 2007; published 22 April 2008)

A novel internal target has been developed, which will make electron scattering off short-lived radioactive nuclei possible in an electron storage ring. An “ion trapping” phenomenon in the electron storage ring was successfully utilized for the first time to form the target for electron scattering. Approximately 7×10^6 stable ^{133}Cs ions were trapped along the electron beam axis for 85 ms at an electron beam current of 80 mA. The collision luminosity between the stored electrons and trapped Cs ions was determined to be $2.4(8) \times 10^{25} \text{ cm}^{-2} \text{ s}^{-1}$ by measuring elastically scattered electrons.

DOI: 10.1103/PhysRevLett.100.164801

PACS numbers: 29.25.Pj, 25.30.Bf, 29.20.db

Size and shape are two of the most fundamental properties of atomic nuclei, and they are essential for the establishment of a nuclear structure model. Indeed, the precise charge density distributions of stable nuclei determined by electron scattering has greatly contributed to the current nuclear structure models. The advancement of accelerator and experimental technologies presently enables us to study the structure of short-lived unstable nuclei far from stability. Peculiar shape structures beyond the models, such as so-called neutron-halo [1] and skin [2] structures, have been discovered.

For the reestablishment of an advanced nuclear structure model widely applicable to nuclei including short-lived nuclei, it is clear that a precise determination of the size and shape of short-lived nuclei is crucial. Electron scattering, which is the best way to study the size and shape, has never been performed for short-lived nuclei, because there has been no method to produce their target. It is, thus, important to establish an experimental method for electron scattering from short-lived nuclei by developing a target production method.

The key of the target development is to achieve large enough luminosities for electron scattering from short-lived nuclei whose production rate is generally small. The luminosity of an order of $10^{27} \text{ cm}^{-2} \text{ s}^{-1}$ is necessary to determine the size and shape of nuclei, i.e., the charge density distribution with ambiguity of several percent or less from measurements of the angular distribution of the elastic scattering cross section [3]. In this Letter, we present the first results from the development of a novel internal target, which will make electron scattering off short-lived nuclei possible.

This new internal target, named SCRIT (self-confining radioactive isotope ion target) [4,5], makes good use of “ion trapping,” a well-known phenomenon in electron storage rings [6–8]. Although ion trapping is a problem

for the stability of the stored electron beam, it allows us to trap ions of interest along the electron beam axis. The SCRIT is a device that localizes ion trapping by applying a longitudinal mirror potential. Because the target ions are confined within a region which is the size of the projectile-electron beam, rather high luminosity is expected using a small number of ions.

A prototype of the SCRIT was installed in the Kaken storage ring (KSR [9]) at Kyoto University. A series of experiments using a stable nucleus, ^{133}Cs , were performed using a 120 MeV electron beam at a current of 80 mA or less.

The SCRIT prototype and the detector system are shown schematically in Fig. 1. Pulsed Cs^{1+} ion beams whose length is $250 \mu\text{s}$ are accelerated vertically to 4.05 keV and are bent 90° into the direction of the beam axis by an electrostatic deflector. The ions, merged with the electron beam at the exit of the deflector, are guided to the SCRIT device using the transverse trapping force provided by the electron beam. The SCRIT device is composed of 40 longitudinally stacked, thin electrodes with 100 mm-long

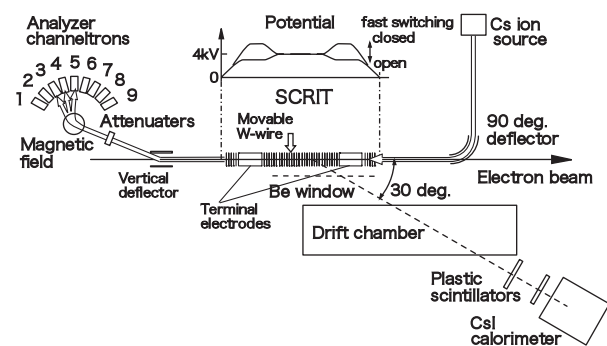


FIG. 1. Prototype of the SCRIT and the experimental setup. Typical form of the mirror potential is shown schematically.

terminals at both ends. They form a longitudinal mirror potential with a 200 mm-long-trapping region in the central region of the SCRIT device. Each electrode has a partial mesh structure to avoid disturbing the scattered electron. The injection and extraction of the ions are manipulated by fast switching of the potential gates. The potential height in the trapping region is tuned so that the kinetic energy of injected ions is below 2 eV. This is essential for preventing fast transverse diffusion caused by the coupling between the longitudinal and transverse motions. Ions in the trapping region are extracted after a certain trapping time. They are guided to an analyzer, which measures the number of trapped ions and their charge-state distribution.

In the analyzer, the ions are separated in a magnetic field and detected with nine channeltrons, No. 1–No. 9 from front to back. The magnetic field is set so that Cs^{1+} ions are detected by channeltron No. 3, $\text{Cs}^{2+,3+}$ ions by No. 4, and $\text{Cs}^{4+,5+,6+}$ ions by No. 5. Attenuator meshes with a total attenuation factor of 10^{-4} are inserted in the beam path of the extracted ions so that the channeltrons can be operated in a pulse counting mode. The overall efficiency of the channeltron is estimated to be 10^{-5} from the attenuation factor, the transmission efficiency of the ions, and the sensitivity of the channeltron.

Scattered electrons emerging from the SCRIT chamber through a 1-mm-thick beryllium window are detected by an electron detection system consisting of a drift chamber, a pair of plastic scintillators, and a calorimeter. The energies and the trajectories of scattered electrons are measured by the calorimeter and the drift chamber, respectively. The calorimeter, consisting of seven pure CsI scintillation crystals, is placed at a scattering angle of 30° and a distance of 1.8 m from the trapping region. Two plastic scintillators are placed between the drift chamber and the calorimeter. One of them, whose size is $120 \times 120 \times 10 \text{ mm}^3$, is placed in front of the calorimeter to define the solid angle. A position-controllable tungsten-wire target of $50 \mu\text{m}$ in diameter is inserted in order to perform an energy calibration of the calorimeter using elastically scattered electrons.

The electron beam was injected into the KSR every 4 s in order to compensate for the short storage lifetime, typically 100 s at 80 mA, and the current was maintained at 75–80 mA. After waiting for the completion of radiation damping, which took 2 s from injection, the measurement was performed during the remaining 2 s. During the measurement, a SCRIT operation cycle composed of injection, trapping, and extraction of the ions was repeated at a frequency of 50 Hz or less. SCRIT operations with and without Cs-ion injection were alternated to provide comparative measurements. The trapping time was varied in the range of 0.25–100 ms and the electron beam current was varied from 50 to 80 mA to measure the time evolution and current dependence of the number of trapped ions. For the measurement of the scattered electrons, the

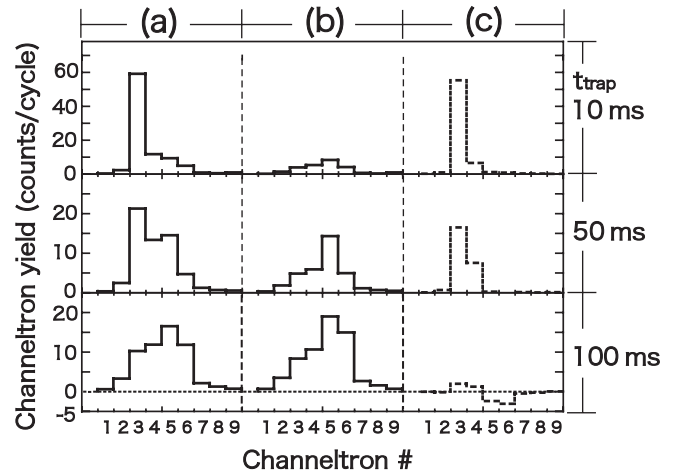


FIG. 2. Typical spectra measured by the analyzer for trapping times of 10, 50, and 100 ms at 75 mA. They are separated into three parts: the spectra (a) with Cs-ion injection, (b) without Cs ions, and (c) the difference (a)–(b). Residual gas ions are expected as: CO_2^+ at channeltron No. 4, CO^+ at No. 5, and H_2O^+ , OH^+ , CH_4^+ , O^+ , C^+ at No. 6.

trapping time was fixed at 20 ms, the SCRIT operation cycle at 33 Hz, and the electron beam current at 75 mA.

Typical spectra of the trapped ions measured by the analyzer are shown in Fig. 2: (a) and (b) represent spectra with and without Cs-ion injection, respectively, and (c) shows their difference. Injected Cs^{1+} ions, observed at channeltron No. 3, are predominant immediately after the injection. As the trapping time increases, the number of Cs ions decreases, as seen in spectra (c), whereas the number of residual gas ions increases, as seen in spectra (b). An interesting behavior of the spectra of trapped Cs ions, seen in spectra (c), is that the abundance of Cs^{2+} and Cs^{3+} ions grows with time due to multiple ionizations by electron impact. This is clear evidence of the interactive collisions between the electron beam and the trapped ions. Another noteworthy phenomenon found in spectra (c) is the negative yields of channeltrons No. 5 and No. 6 for the 100-ms trapping time. This may be a result of evaporative cooling, which is well established in the electron beam ion trap (EBIT) [10,11]. When the ion density increases, light gas ions are evaporated due to energy-exchange collisions with heavier ions, Cs ions, in particular. Consequently, the growth rate of lighter residual gas ions is reduced due to the existence of the Cs ions.

The number of trapped Cs ions, $N(t_{\text{trap}})$, including all charge states is shown in Fig. 3(a) as a function of the trapping time, t_{trap} . A decay curve of the form is fitted to the data, where the number of initially trapped Cs ions, N_i , and the trapping lifetime, τ_{life} , are fitting parameters. They are plotted as a function of the electron beam current in Fig. 3(b). The number of trapped ions, N_i , increases linearly with current, and it is 7×10^6 at 75–80 mA. This linearity is due to the fact that the acceptable transverse

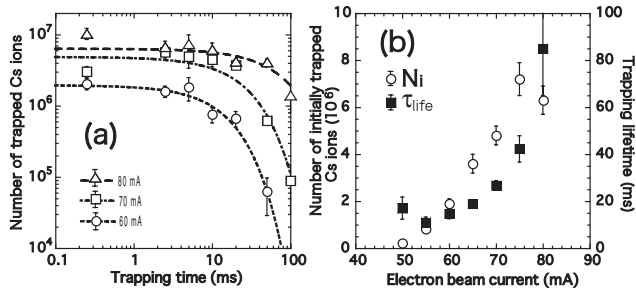


FIG. 3. (a) Time evolution of the number of trapped Cs ions together with fitted decay curves and (b) current dependencies of the fitting parameters N_i and τ_{life} .

phase volume provided by the electron beam is proportional to the current. On the other hand, the trapping lifetime increases exponentially and reaches 85 ms at 80 mA. An increase of highly charged ions extends the trapping lifetime because they feel a deeper potential well; in addition, the evaporative cooling effect also helps to achieve longer trapping lifetime.

The time evolution of the trapped Cs ions is well reproduced by a calculation, which solves the rate equations proposed for the EBIT by Penetrante *et al.* [12], as shown in Fig. 4. Details of the calculation are described in Refs. [4,12]. This shows that, within the present trapping-time range, the ion trapping phenomenon in a high-energy electron storage ring can be treated similarly to the EBIT. The collision luminosity plotted in the figure is calculated to reproduce the ratio of $(Cs^{2+} + Cs^{3+})/Cs^{1+}$; it exceeds $10^{25} \text{ cm}^{-2} \text{ s}^{-1}$ even at a 50 ms trapping time.

For precise luminosity determination, elastically scattered electrons from the trapped ions were measured. Figure 5 shows (a) the vertex distribution of scattered electrons measured using the drift chamber and (b) electron energy spectra measured using the calorimeter. The vertex is defined as the intersection of the electron

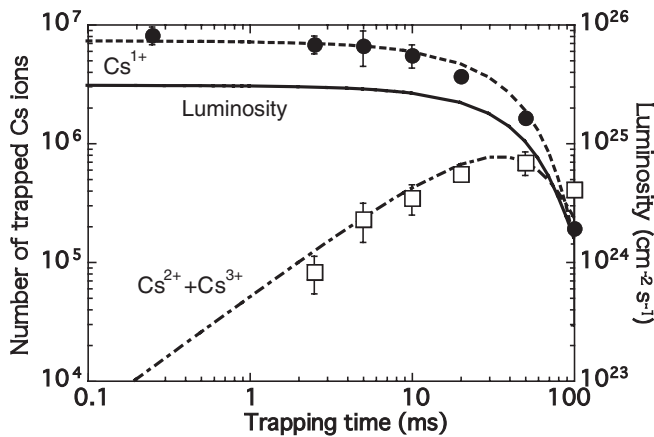


FIG. 4. Calculations reproducing the time evolution of trapped Cs^{1+} (dotted curve), $Cs^{2+} + Cs^{3+}$ (dash-dotted curve) ions, and the estimated luminosity (solid curve) at 75 mA.

beam axis and the trajectory of the scattered electron. The origin of the vertex coordinate is defined as the center of the SCRIT device. Vertices of the events above 80 MeV in (b) are selected and shown in (a). A clear enhancement only seen in the trapping region is due to the trapped ions. On the other hand, the peaks at around -300 and 200 mm, which are due to electrons from the terminal electrodes, are almost identical for measurements with and without Cs ions. They should be due to the beam halos.

Figure 5(b) shows the energy distributions of events whose vertices are located in the trapping region. The spectra with and without Cs ions are almost identical below approximately 80 MeV, whereas a clear enhancement due to the ions is observed at around 120 MeV. A subtracted energy spectrum and the response of the calorimeter to 120 MeV electrons are plotted together in (b). The position and the shape of the subtracted spectrum are consistent with the response.

Here we should briefly mention the energy spectrum in lower energy region, below about 80 MeV. A GEANT simulation, which fully takes into account the geometry of the SCRIT prototype, reproduces the energy dependence of the spectrum in this energy region. The simulation assumes that (i) beam halos produce electromagnetic showers in materials, such as the SCRIT electrodes, and (ii) the shower-produced low-energy electrons (positrons) from the trapping region are detected by the calorimeter. These assumptions are reasonable because it is known from the short storage lifetime of the KSR that in the order of 10^8 electrons are lost every second, and a part of them definitely produces showers in the materials. No difference, therefore, is expected whether the Cs ions are trapped or not, since no effects of Cs-ion trapping were observed for the storage lifetime.

From the clear differences seen in the vertex distribution and the energy spectrum, it is certain that electrons scattered from trapped Cs ions were observed. In addition, the agreement of the energy spectrum with that of the detector

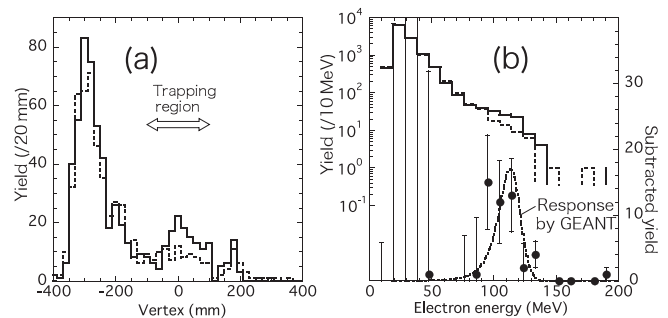


FIG. 5. (a) Vertex distribution of scattered electrons and (b) the energy spectrum. Solid (dotted) line in both figures indicates the data with (without) Cs-ion trapping. In (b), closed circles show subtracted spectrum and the dash-dotted line is the response of the calorimeter to 120 MeV electrons reproduced by a GEANT simulation.

response to 120 MeV electrons leads us to conclude that they are from elastic scattering. Note that the electrons scattered from the ions can be safely assumed to be those from elastic scattering because of the low momentum transfer, 60 MeV/c, under the present kinematics.

The total number of events which were determined to be elastic scattering from trapped Cs ions is 47(15) for a net measurement time of 1.2 hours. Using the elastic scattering cross section calculated by a distorted wave calculation code, DREPHA [13], the averaged luminosity is estimated to be $2.4(8) \times 10^{25} \text{ cm}^{-2} \text{ s}^{-1}$. Since we do not know of any elastic electron scattering data for Cs, the parameters for the Cs charge distribution used in the calculation are obtained by scaling the parameters of neighboring nuclei [14]. The associated error in the cross section is estimated to be less than 5%. The effects of the vertex distribution and the finite size of the detector are taken into account, and the radiative correction is also applied. This luminosity is consistent with that estimated from the measurement of the time evolution of the trapped Cs ions as shown in Fig. 4.

In the present experiment, we succeeded in developing a novel internal target, SCRIT, utilizing ion trapping in an electron storage ring. Approximately 7×10^6 Cs ions were trapped in the SCRIT device for a duration of 85 ms at 80 mA, and the luminosity was determined to be $2.4(8) \times 10^{25} \text{ cm}^{-2} \text{ s}^{-1}$ from the measurement elastic scattering events. Experimental data show that both the number of trapped ions and the trapping lifetime can be improved by increasing the electron beam current. Extrapolating present data using the calculation, which reproduces time evolution of trapped ions, it is predicted at several hundreds mA of the current that approximately 10^8 ions are trapped for a much longer time and the luminosity of more than $10^{27} \text{ cm}^{-2} \text{ s}^{-1}$ is achieved. Therefore, we conclude that a SCRIT is feasible as a target for electron scattering experiments, and it is a candidate method for making possible electron scattering experiments on short-lived radioactive nuclei. An expected experimental system using the SCRIT will be much more compact than the electron-ion collider system [15] and be used at low-energy RI-beam facilities.

The authors would like to thank M. Ishihara for many useful discussions and N. Nakamura for providing technical information on the electron beam ion trap (EBIT).

*Present address: Institute for Semiconductor Technology, ULVAC Co., Ltd., Susono, Shizuoka 410-1231, Japan.

†Present address: Accelerator Laboratory, High Energy Accelerator Research Organization (KEK), Tsukuba, Ibaraki 305-0801, Japan.

‡Present address: Department of Complexity Science and Engineering, University of Tokyo, Kashiwa, Chiba 277-8583, Japan.

- [1] I. Tanihata *et al.*, Phys. Rev. Lett. **55**, 2676 (1985).
- [2] T. Suzuki *et al.*, Phys. Rev. Lett. **75**, 3241 (1995).
- [3] T. Suda and M. Wakasygi, Prog. Part. Nucl. Phys. **55**, 417 (2005).
- [4] M. Wakasugi, T. Suda, and Y. Yano, Nucl. Instrum. Methods Phys. Res., Sect. A **532**, 216 (2004).
- [5] Y. Yano, Nucl. Instrum. Methods Phys. Res., Sect. B **261**, 1009 (2007).
- [6] L.J. Laslett, A.M. Sessler, and D. Möhl, Nucl. Instrum. Methods **121**, 517 (1974).
- [7] M. Q. Barton, Nucl. Instrum. Methods Phys. Res., Sect. A **243**, 278 (1986).
- [8] C.J. Bocchetta and A. Wrulich, Nucl. Instrum. Methods Phys. Res., Sect. A **278**, 807 (1989).
- [9] A. Noda *et al.*, in *Proceedings of the Fifth European Particle Accelerator Conference, Barcelona, 1996*, edited by S. Myers *et al.* (Institute of Physics, Bristol, U.K., 1996), p. 451.
- [10] M.B. Schneider, M.A. Levine, C.L. Bennett, J.R. Henderson, D.A. Knapp, and R.E. Marrs, in *Proceedings of the International Symposium on Electron Beam Ion Source and Their Applications*, edited by A. Hershcovitch, AIP Conf. Proc. No. 188 (AIP, New York, 1989), p. 158.
- [11] B.M. Penetrante, J.N. Bardsley, M.A. Levine, D.A. Knapp, and R.E. Marrs, Phys. Rev. A **43**, 4873 (1991).
- [12] B.M. Penetrante, J.N. Bardsley, D. DeWitt, M. Clark, and D. Schneider, Phys. Rev. A **43**, 4861 (1991).
- [13] DREPHA, phase shift code for the calculation of elastic scattering, B. Dreher and J. Friedrich (private communication).
- [14] H. de Vries, W.W. de Jagaer, and C. de Vries, At. Data Nucl. Data Tables **36**, 495 (1987).
- [15] H. Geissel *et al.*, Nucl. Instrum. Methods Phys. Res., Sect. B **204**, 71 (2003).